Polymer Multilayers with pH-Triggered Release of Antibacterial Agents

ARTICLE *in* BIOMACROMOLECULES · OCTOBER 2010

Impact Factor: 5.75 · DOI: 10.1021/bm100975w · Source: PubMed

5 AUTHORS, INCLUDING:

Svetlana Pavlukhina
Stevens Institute of Technology
13 PUBLICATIONS **219** CITATIONS
SEE PROFILE

Svetlana Sukhishvili
Stevens Institute of Technology
134 PUBLICATIONS **4,812** CITATIONS
SEE PROFILE

Polymer Multilayers with pH-Triggered Release of Antibacterial Agents

Svetlana Pavlukhina,[†] Yiming Lu,[†] Altida Patimetha,[‡] Matthew Libera,[‡] and Svetlana Sukhishvili*[,†]

Department of Chemistry, Chemical Biology and Biomedical Engineering and Department of Chemical Engineering and Materials Science, Stevens Institute of Technology, Hoboken, New Jersey 07030, United States

Received August 19, 2010; Revised Manuscript Received October 9, 2010

We report on the layer-by-layer design principles of poly(methacrylic acid) (PMAA) ultrathin hydrogel coatings that release antimicrobial agents (AmAs) in response to pH variations. The studied AmAs include gentamicin and an antibacterial cationic peptide L5. Adipic acid dihydrazide (AADH) is a cross-linker which, relative to ethylenediamine (EDA), increases the hydrogel hydrophobicity and introduces centers for hydrogen bonding to AmAs. AmA retention in AADH-cross-linked hydrogels in high-salt solutions was enhanced while AmA release at low pH was suppressed. L5 retains its antibacterial activity toward planktonic *Staphylococcus epidermidis* after release from PMAA hydrogels in response to pH decreases in the surrounding medium due to bacterial growth. *Staphylococcus epidermidis* adhesion and colonization was almost completely inhibited by L5 loading of hydrogels. The AmA-releasing and AmA-retaining properties of these hydrogel coatings provide new opportunities to study the fundamental mechanisms of AmA-coating−bacteria interactions and develop a new class of clinically relevant antibacterial coatings for medical devices.

Introduction

The susceptibility of implantable biomedical devices to bacterial colonization and the resulting infection of surrounding tissue can catastrophically compromise device performance and lead to high treatment costs, significant patient discomfort, and increased morbidity.[1,2] Such biomaterial-associated infection is often linked to bacterial biofilms that consist of bacteria organized into communities with functional heterogeneity enclosed in a self-produced extracellular matrix.[3,4] When in the biofilm state, bacteria become orders of magnitude more resistant to antibiotics than bacteria in the planktonic state.[5−9] In many cases, the only solution is to remove the implanted medical device, resolve the infection, and pursue a revision surgery with a second implant.

One promising approach to inhibit biofilm growth is the creation of functional antibacterial surface coatings.[10−13] Polymers in antibacterial coatings can either directly work as cationic agents with a bacteria-killing ability,[14] or they can serve as matrices for the delivery of other antibacterial molecules, such as silver ions or antibiotics.[15] There are several approaches to design antibacterial coatings, including the creation of surfaces that resist bacterial adhesion,[16−19] kill bacteria upon contact,[13,20] or leach antibacterial agents.[20,21] Antibacterial coatings that leach drugs can, however, suffer from the fact that the local drug concentration decreases with the elution time, and the coatings lose their antibacterial activity when the concentration of the antimicrobial agent falls below the minimum inhibitory concentration (MIC). Therefore, nonleaching coatings designed to provide long-term protection against bacterial adhesion and colonization are also being explored.

Functionalization of surfaces can involve adsorption of water-soluble polymers at a substrate to form a polymer monolayer, tethering of polymer chains to form brushes,[16,17,22] or the alternating deposition of monolayers of different polymer types to form multilayer films.[23] One attractive feature of the latter approach is the degree of flexibility with which to control the structure and properties of the resulting polyelectrolyte multilayer (PEM) film. The film thickness, for example, can be controlled by varying the number of deposited layers, and the thickness of the individual self-assembled polymer layers can be controlled through the deposition conditions such as pH and ionic strength.[24,25] Layer-by-layer (LbL) self-assembled films can incorporate a variety of functional biomolecules, including proteins, enzymes, and polysaccharides, often without a significant decrease in the biomolecule activity.[26] Specifically important for the application of LbL technology to the modification of implant surfaces is the capability of depositing a conformal coating on a substrate of virtually any shape, as well as the ability to deposit films at any inner surface accessible to solvent, in a non-line-of-sight fashion. In addition, the LbL technique enables careful control of the film composition, stiffness,[27] and compliance,[28] all of which are critical parameters in designing antibacterial coatings.

The potential of PEM films as antibacterial coatings has been explored by several groups. For example, antimicrobial agents (silver nitrate or cetrimide) were introduced within PEMs by codissolving with branched poly(ethyleneimine) (BPEI) for alternating deposition with poly(acrylic acid) (PAA) solutions.[29] Amphiphilic block copolymer micelles of poly(ethylene oxide)-*block*-poly(ε-caprolactone) were also used as a carrier of hydrophobic antibacterial drug triclosan.[30] The micelles were self-assembled within LbL films using the hydrogen bonding between the polyethylene oxide (PEO) micelle corona and PAA. By changing the environment to a physiologically relevant pH, the film was deconstructed to release the micelles, and the deconstruction rate could be controlled by thermal cross-linking of the film.[30] An amphiphilic linear−dendritic triblock copolymer of poly(amidoamine)/(poly(propylene glycol) bis(2-aminopropyl ether) (PPO) has also been used as a vehicle to enable the burst delivery of triclosan from surfaces.[31] Another strategy to endow LbL films with antimicrobial properties is the

* To whom correspondence should be addressed. E-mail: ssukhish@stevens.edu.
[†] Department of Chemistry, Chemical Biology and Biomedical Engineering.
[‡] Department of Chemical Engineering and Materials Science.

10.1021/bm100975w
Published on Web 10/28/2010

incorporation of a water-soluble precursor of titanium dioxide, which produces TiO_2 nanoparticles, yielding films that release active antibacterial superoxide anions and hydrogen peroxide species in close proximity to the active coating.[32] Antibacterial gentamicin-containing LbL films were also constructed from hydrolytically degradable poly(β-amino ester) and hyaluronic acid (HA) or PAA.[33,34] Released by diffusion and film erosion, the gentamicin was effective in inhibiting the growth of *S. aureus* and was benign for MC3T3 osteoblast cells.[33,34] Nonleaching LbL coatings of single-wall carbon nanotube (SWNT), lysozyme, and DNA with antimicrobial activity have also been reported.[35] Long-term antibacterial properties of hyaluronic acid (HA) and chitoson (CH) on Ti, coupled with surface-immobilized, cell-adhesive arginine−glycine−aspartic acid (RGD) peptide have also been demonstrated.[36] Examples of antibacterial surfaces acting through several mechanisms have also been reported. Rubner and co-workers have constructed PEM films of poly(allylamine) hydrochloride (PAH) and PAA, which leach antibacterial Ag^+ ions, and also kill on contact with the surface with immobilized quaternary ammonium salts.[37] Another multifunctional LbL coating composed of chitosan−silver nitrate complex and heparin with combined contact-killing and antibacterial-leaching capabilities has been recently described by Shen and co-workers.[38] In this case, the chitosan killed bacteria upon their contact with the surface, while silver ions acted against bacteria in solution. Another approach includes assembly of TiO_2−chitosan/heparin multilayers loaded with nanosilver. Such films have demonstrated a dual mechanism of action, having bactericidal properties against *E. coli* in the dark due to elution of silver ions and enhanced antibacterial properties in UV light due to the presence of TiO_2 nanoparticles.[39]

Broad spectrum antibiotics, such as gentamicin and others, have been explored to combat biofilm growth. These have an advantage because of their long-term stability. Antimicrobial polypeptides (AmPs), however, have an advantage over traditional antibiotics, as they usually are not associated with the development of antimicrobial resistance.[40] The low capability of AmPs to develop bacterial resistance is thought to be due to the general mechanism of AmP binding with bacterial walls, leading to the formation of membrane pores.[41] AmPs have been used to efficiently combat the biofilm growth.[42] They have a broad spectrum of action and hold their activity against gram-positive, gram-negative, and multidrug-resistant bacteria, fungi, and viruses.[43] AmPs have been incorporated within LbL films. Noneluting nondegradable films were constructed using antibacterial and antifungal AmPs.[44,45] Ponericin G1, an AmP highly potent against *S. aureus*, has also been incorporated within a hydrolytically degradable PEM achieving high loadings, inhibition of bacterial attachment, as well as prolonged release over 10 days.[46] A negatively charged polyelectrolyte complex was also formed through binding of a hydrophobic peptide gramicidin A from *Bacillus brevis* with an amphiphilic polysaccharide, and the complex was subsequently assembled with cationic poly(L-lysine).[26] The resulting films inhibited attachment of the gram-positive bacterium *Enterococcus faecalis* as well as eluted the AmPs in solution.[26]

Along with noneluting and continuously eluting antibacterial coatings, polymer matrices that can release their load in response to the environmental stimuli such as pH, ionic strength, temperature, electric, or magnetic field have been studied.[47−52] In particular, we have previously reported on ultrathin single-component poly(methacrylic acid) (PMAA) hydrogels which were stable over a wide pH range.[53] The hydrogels were produced by the selective cross-linking of PMAA within hydrogen-bonded multilayers using ethylenediamine (EDA), and we demonstrated their use for pH-controlled loading and release of model cationic dyes and proteins.[53] In this paper, we (1) explore the potential of such coatings to retain and release potent antibacterial agents (AmAs) such as gentamicin and an antibacterial peptide; (2) modulate the binding strength of the AmAs to the hydrogel coatings in salt solutions by introducing an alternate cross-linker; and (3) explore and contrast the ability of these coatings to kill bacteria at surfaces and in solution. We chose to work with *Staphylococcus epidermidis* (*S. epidermidis*) as this bacterium readily forms biofilms[54,55] and is frequently implicated in implanted medical device related infections.[56] The central idea of this work is to use pH variations associated with growth of *S. epidermidis* as an internal trigger to release AmAs from surface coatings.

Experimental Section

Materials. Poly(methacrylic acid) (PMAA; M_w 150 kDa), poly(*N*-vinyl pyrrolidone) (PVPON; M_w 2500), gentamicin (10 mg/mL in H_2O), lysozyme, monobasic and dibasic sodium phosphate, *N*-hydroxysulfosuccinimide sodium salt, 1-ethyl-3-(3-dimethylaminopropyl) carbodiimide hydrochloride (CDI), ethylenediamine (EDA), adipic acid dihydrazide (AADH), hydrochloric acid, sodium hydroxide, sodium chloride, and phosphate buffer saline (PBS; powder, pH 7.4, 0.138 M NaCl; 0.0027 M KCl in 0.01 M phosphate buffer) were purchased from Sigma Aldrich. All chemicals were used without any further purification. Tryptic soy broth (TSB) was purchased from MP Biomedicals. Inc. Yeast extract was from Acros Organics. Peptide L5 with the chemical structure shown in Scheme 1 and with 95.1% purity was synthesized by Gen Script (Piscataway, NJ). Millipore (Milli-Q system) filtered water with a resistivity of 18.2 MΩ was used in all experiments. D_2O with 99.9% isotope content was purchased from Cambridge Isotope Laboratories and was used as received. Silicon (110) wafers were prime grade, p-type, 500 μm thick, with native oxide layer ~2 nm thick, and were bought from University Wafer. Trypticase Soy Agar plates with 5% Sheep Blood were bought from Becton, Dickinson and Company (Cat. No. 221261). The plates were stored at 4 °C. The strain of *Staphylococcus epidermidis* (NJ9709; *S. epidermidis*) was isolated from the surfaces of infected intravenous catheters from a patient at University Hospital, Newark, NJ, and provided to Stevens by Prof. Jeff Kaplan.[57]

Deposition of Precursor Layer. Hydrogels were deposited onto the surfaces of silicon wafers, which were precleaned under a quartz UV lamp, soaked in concentrated sulfuric acid, and then carefully rinsed with Milli-Q water. To enhance the attachment of multilayers to the silica surface, two bilayers of BPEI/PMAA were deposited as a precursor. BPEI and PMAA were allowed to sequentially adsorb at the surface from 0.2 mg/mL polymer solutions in 0.01 M phosphate buffer at pH 5. Each deposition step was followed by rinsing with buffer solution at the same pH value. The precursor film was then stabilized by thermal cross-linking in an oven at 125 °C for 1 h. The thickness of the precursor layer was 9 ± 1 nm. While in situ ellipsometry data on film swelling are reported for hydrogel films including the precursor layer, this thickness has been subtracted from all ellipsometric measurements of dry films and also subtracted from the film thickness in the calculation of the swelling ratio of hydrated films.

Preparation of AADH- and EDA-Cross-Linked PMAA Surface Hydrogels. Deposition of hydrogen-bonded PVPON/PMAA multilayers at the surface of the precursor-coated substrates was performed as described earlier[53] using 0.2 mg/mL polymer solutions at pH 2. Polymers were allowed to adsorb for 15 min and two rinsing steps with a buffer at pH 2 were applied after each deposition step. After the desired number of bilayers was deposited, the film was chemically cross-linked. The cross-linking procedure included activation of carboxylic groups in a solution containing CDI (3 mg/mL) in 0.01 M phosphate buffer at pH 5.2 for 20 min and subsequent treatment with a cross-linker solution of AADH (9 mg/mL, pH 4) or EDA (3 mg/mL, pH 5.2). To remove PVPON and the activation agents, cross-linked multilayers were exposed to a 0.01 M phosphate buffer solution at pH

Scheme 1. Chemical Structures of Polymers (PVPON and PMAA), Cross-Linking Agents (EDA and AADH), and Antibacterial Molecules (Lysozyme, Gentamicin, and Peptide L5)

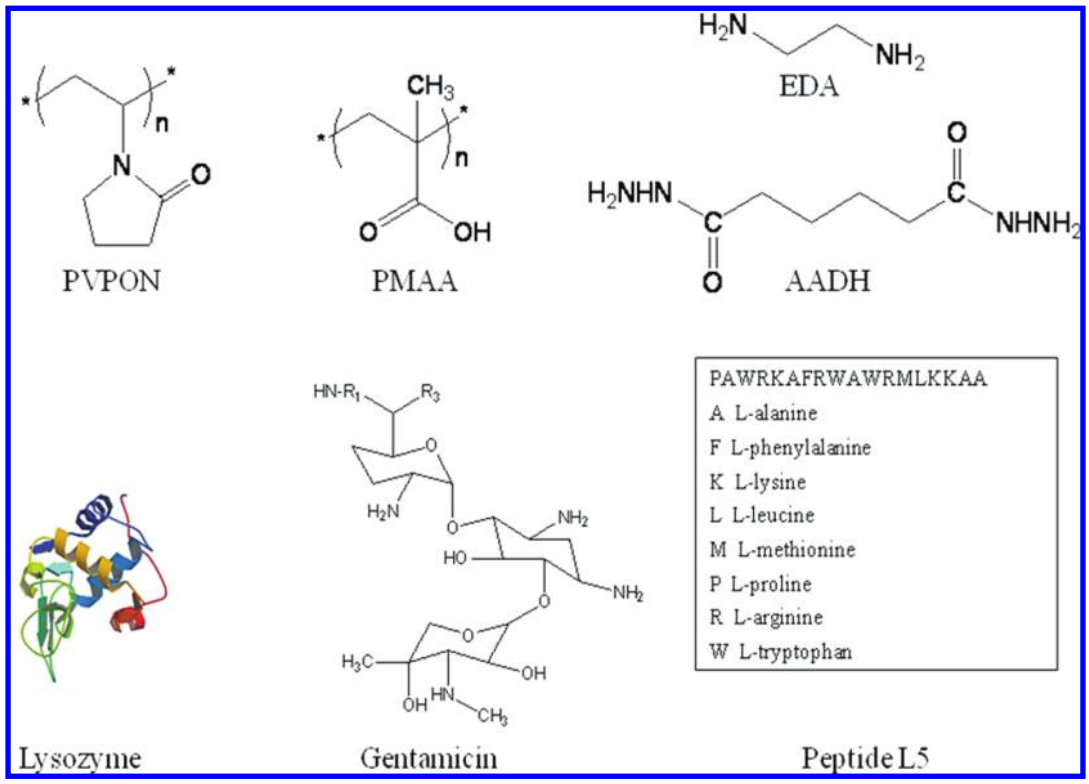

7.5 for 2 h. Finally, the hydrogels were rinsed with pure water and dried under flowing nitrogen gas.

Incorporation of AmAs within PMAA Films. To load AmAs, PMAA hydrogels cross-linked with EDA or AADH were exposed to solutions of the following compounds: lysozyme (0.1 mg/mL in 0.01 M phosphate buffer at pH 7.5, 0.6 mL), gentamicin (1 mg/mL in 0.01 M phosphate buffer at pH 7.5, 0.6 mL) or peptide L5 (100 μM in 0.01 M phosphate buffer at pH 7.5, 0.6 mL) for 20 min to achieve complete absorption within the films.

Release of AmAs from PMAA Films Triggered by Ionic Strength or pH. To study release of AmAs as a function of ionic strength, PMAA hydrogel films were exposed to 0.01 M phosphate buffer solutions which additionally contained various concentrations of NaCl. For studies of pH-triggered release, PMAA hydrogel films were exposed to 0.01 M phosphate buffer solutions containing 0.2 M NaCl with pH set at various values between 5.0 and 7.5.

ATR-FTIR Spectroscopy. In situ ATR-FTIR experiments were performed with a Bruker Equinox-55 Fourier transform infrared spectrometer equipped with a narrow-band mercury cadmium telluride detector. The ATR Si crystal (50 × 20 × 2 mm, cut at 45°, Harrick Scientific) was installed within a flow-through stainless steel cell filled with D_2O solutions.

Phase-Modulated Ellipsometry Measurements of Dry and Swollen Films. Ellipsometry measurements were performed using a home-built, single-wavelength, phase-modulated ellipsometer at 65° of incidence.[58] Optical properties of the substrates and oxide layer thickness were determined prior to polymer deposition. In measurements of dry film thickness, the refractive index was fixed at a value of 1.5.

Measurements of PMAA hydrogel swelling were performed in situ using a custom-made cylindrical flow-through glass cell. To obtain the swollen film thickness, the cell was filled with 0.01 M phosphate buffer at various pH values, and measurements were taken after the hydrogel was allowed to equilibrate for 20 min. The ellipsometry setup and procedures used in swelling measurements are described elsewhere.[58]

Preparation of *S. epidermidis* Inocula. An isolated bacterial colony taken from an agar plate was transferred to a 100-mm-diameter polystyrene Petri dish (Corning No. 430167) containing 20 mL of growth medium. Growth medium consisted of TSB (containing ~0.09 M NaCl and ~0.014 M K_2HPO_4, 17 g/L casein peptone, 2.5 g/L dextrose, and 3 g/L soya peptone) supplemented with 6 g of yeast extract and 8 g of glucose per liter. The cultures were incubated at 37 °C for 18 h under static conditions. The biofilm from the bottom of the dish was washed with PBS three times and scraped into 3 mL of TSB by using a cell scraper. The aggregates of cells were transferred to a 15 mL polypropylene centrifuge tube, where they were disrupted by a high-speed vortex agitation for 30 s followed by sonication for 30 s. The bacterial suspension was then filtered using a 2 μm filter (Millipore) to remove cell clusters larger than 1 colony forming unit (CFU). The resulting inoculum contained around 10^8 colony-forming units (CFU) per mL of growth medium, as determined by counting the bacteria with a counting chamber for bacteria (Petroff Hausser Counting Chamber, No. 3900).

Determination of Minimum Inhibitory Concentration (MIC). A total of 75 μL of diluted peptide L5 solutions with a concentration of 1, 2, 2.5, 5, 10, 25, 50, 75, or 100 μM/mL were added to a 96-well sterile microtiter tray to two rows of wells. Then, 75 μL of *S. epidermidis* inoculum with a final concentration of 10^5 CFU/mL was added to the second row of the wells. To check the sterility and adequacy of the bacterium suspension, uninoculated and inoculated antibiotic-free wells were included. The trays were incubated at 37 °C for 18−20 h in air. The MIC was determined as the lowest concentration of antibiotic at which no visible growth occurred.[59]

Quantification of *S. epidermidis* Growth in Solutions and at Surfaces. Silicon wafers containing hydrogel coatings were placed in test tubes filled with a mixture of 100−150 μL of inoculum and 2 mL of TSB. The samples were incubated at 37 °C for 4 h. For the experiments in solutions, solution-immersed wafers were sonicated for 3 min after incubation to remove loosely attached bacteria. Then, the optical density of cell suspensions at 600 nm was determined using a UV/vis Spectrometer Lambda 40. For the experiments on the surfaces, optical imaging was performed using a Nikon Eclipse E1000 microscope. Nine images were analyzed for each EDA- and AADH-cross-linked loaded and unloaded sample. The fixing procedure was performed by exposing the substrates to 4% paraformaldehyde for 20 min.

Scheme 2. Procedure for Preparation of Functional Antibacterial Films

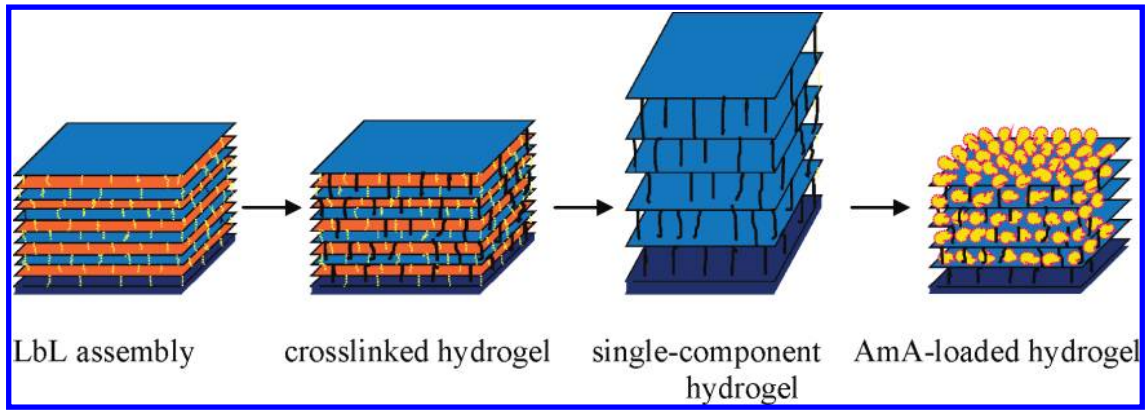

Results and Discussion

Preparation of PMAA Hydrogel. Schemes 1 and 2 show the chemical structures of the polymers, cross-linkers, and AmAs, as well as the procedure for preparation of AmA-loaded hydrogel thin films. While the PVPON/PMAA hydrogen-bonded LbL films used for hydrogel preparation were the same as in our prior work,[53] important differences were introduced via the use of EDA or AADH cross-linker. In particular, AADH is more hydrophobic, and the amide bonds in its structure enable additional hydrogen bonding with AmAs. Peptide L5 is a derivative of the N-terminal helical region of bovine lactoferrin peptide. This peptide has been reported to be highly active against *Escherichia coli* and *Staphylococcus aureus*, with an MIC of 4.5 μg/mL (2 μM) against these bacteria.[60] Gentamicin is a broad-spectrum antibiotic clinically used for the treatment of implant-related infections. The MIC of L5 and gentamicin against *S. epidermidis* determined in this work were 45 μg/mL and 128 μg/mL, respectively. At physiological pH, gentamicin and L5 are positively charged, leading to electrostatic interactions of these AmAs with the PMAA hydrogel matrix. However, these interactions are modulated by the presence of -CO-NH- groups in the AADH molecule, which provide centers for hydrogen bonding between carbonyl groups of AADH amide moieties and hydrogen-donating groups in an AmA. In addition, the use of AADH cross-linker with a pK_a of the hydrazide group lower than that of the primary amino group, favors the cross-linking reaction because of a weaker protonation of the reacting groups. The difference in pK_a between hydrazide (pK_a = 2.5)[61] and the primary amino group (pK_a > 9) contributes to the selective attachment of hydrazide rather than amine to CDI-activated carboxylic groups at neutral and acidic pH values. AADH cross-linker can therefore be used to cross-link hydrogen-bonded multilayers with a critical disintegration pH significantly lower than that for PVPON/PMAA system.

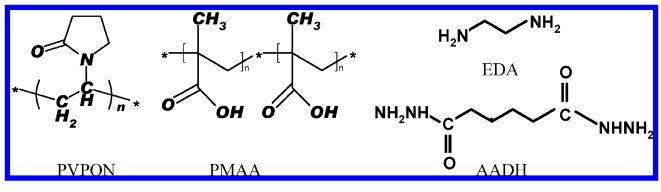

Release of the PVPON from the PVPON/PMAA films of 1, 5, and 10 bilayers was monitored by ellipsometry. The dry thickness of 10 bilayers deposited at pH 2 was 57 ± 3 nm (including 9 nm of the BPEI/PMAA precursor layer). After cross-linking with AADH or EDA the films were exposed to pH 7.5 for 2 h to remove the PVPON and the activation agents. The dry film thickness decreased to 39 ± 3 nm for both the AADH- and EDA-cross-linked systems. After accounting for the thickness of the precursor layer, such a decrease in the dry thickness is consistent with a complete release of PVPON.

We used ATR-FTIR to further confirm the successful cross-linking of PMAA layers with AADH and the complete release of PVPON. The FTIR spectra of $(PVPON/PMAA)_5$ films and the cross-linked hydrogel are shown in Figure S2 in the Supporting Information. The assignment of peaks was similar to EDA-cross-linked PMAA hydrogels reported by our group earlier.[53] Cross-linking of $(PVPON/PMAA)_5$ films with AADH was monitored by the appearance of a carbonyl stretching vibration for reacted hydrazide groups -CO-NH-NH-CO- at 1756 cm^{-1}.

Swelling of PMAA LbL Hydrogels: In Situ Ellipsometry. AADH and EDA cross-linked $(PMAA)_{10}$ hydrogels, formed after a complete removal of PVPON from cross-linked $(PVPON/PMAA)_{10}$ films, were used for in situ ellipsometry experiments. The swelling ratio of hydrogels in solutions was defined as the difference between the wet and dry film thickness divided by the dry film thickness. The swelling ratios and the refractive indices of EDA-cross-linked hydrogels were reported by our group earlier.[53] The swelling profiles of both types of hydrogels and their refractive indices are shown in Figure 1.

Both types of hydrogels demonstrated increased swelling at pH > 5.5 due to deprotonation and the resulting repulsion between ionized carboxylic groups. In contrast to EDA-cross-linked hydrogels, which also swelled at pH < 5.5 due to the protonation of free primary amino groups of a one-end-attached EDA (see Figure 1, panel B), AADH-cross-linked hydrogels did not swell at low pH. This is likely due to the higher reactivity and the longer length of AADH, both ends of which can bind to the PMAA hydrogel matrix, as well as due to its low pK_a value (pK_a = 2.5).[61] Panels A and B of Figure 1 also demonstrate that in 0.2 M NaCl solutions, the swelling ratio in both types of hydrogels remained the same as in low-salt solutions, but the swelling profiles shifted to lower values of pH. This is probably the result of a salt-induced increase in the degree of ionization of carboxylic groups of hydrogel matrix — a phenomenon often observed with weak polyelectrolytes.[62] Figure 1 also shows changes of the refractive indices for swollen/deswollen hydrogels, where higher swelling ratios correspond to lower refractive indices. The hydrogel swelling behavior was reproducible and reversible upon changes in pH and ionic strength. The cross-link density of PMAA hydrogel with EDA was calculated from the swelling data at pH 5 using the Flory equation for the one-dimensional swelling of nonionic

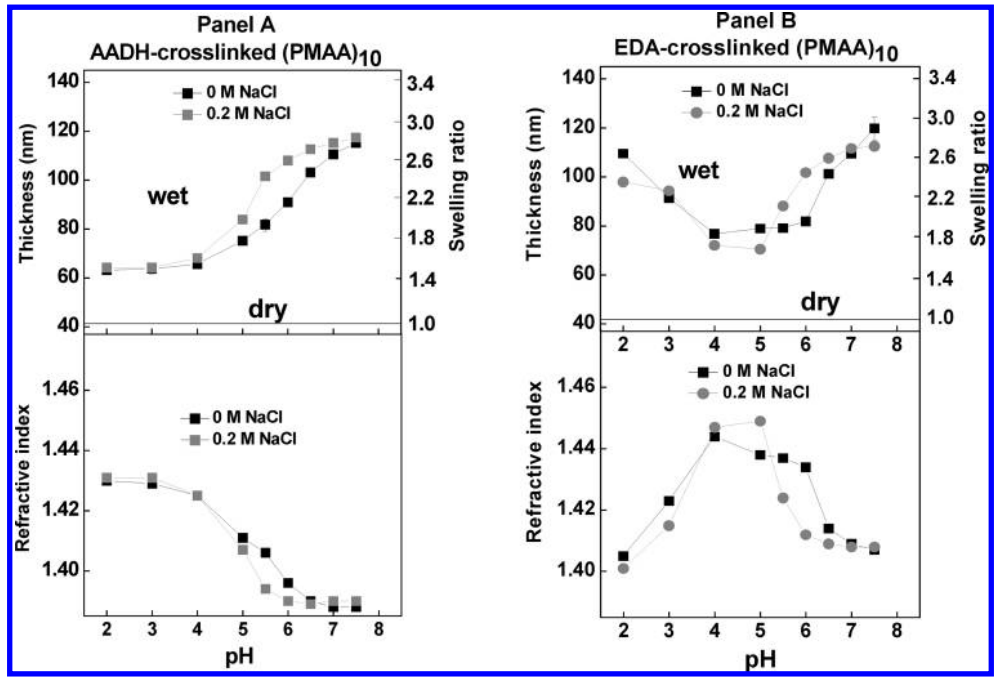

Figure 1. Swelling ratios and refractive indices of $(PMAA)_{10}$ films cross-linked with AADH (panel A) and EDA (panel B) as a function of pH supported by 0.01 M phosphate buffer with and without 0.2 M NaCl, as measured by in situ ellipsometry. For both EDA- and AADH-cross-linked hydrogels, the dry thickness was ~41 nm, including a 9 nm precursor layer.

gels.[63] This calculation yielded an estimate of 15 PMAA monomer units or 30 C−C bonds between the cross-links. Based on this value, we estimated the mesh size of the hydrogel using the procedure described earlier.[63] The mesh size for swollen hydrogel was calculated to be ~3.4 nm at pH 5. At pH 7.5, where PMAA units become ionized, the hydrogel size is further increased, allowing transport of antibacterial agents, including Lys globules with deminsion 3 × 3 × 4.5 nm, through the hydrogel matrix. We could not perform a similar calculation for the AADH-cross-linked hydrogel, because of the significant contribution of the cross-linker length to the mesh size. However, longer cross-links should allow ready permeation of AmAs into the hydrogels even at higher cross-linking densities.

Inclusion of Antibacterial Agents. The resulting films were then loaded with guest molecules, lysozyme, gentamicin, and peptide L5, whose structures are shown in Scheme 1. Loading and release of lysozyme within EDA-cross-linked PMAA surface hydrogel has been reported in an earlier paper.[53] Lysozyme has a M_w of 14.6 kDa, and its isoelectric point is about 11.0. It carries eight positive charges at pH 7.4.[64,65] Gentamicin is an aminoglycoside antibiotic, effective against most gram-positive and gram-negative bacteria. Aminoglycosides have a multiple effect on the bacteria including inhibition of protein synthesis by binding to the 30S ribosomal subunit. This binding prevents the formation of an initiation complex with mRNA, resulting in the misreading of the mRNA. Inhibited protein synthesis ultimately leads to an enhanced membrane leakage. Gentamicin has a pK_a of 8.6 and it has three positive charges at pH 7.5.[66] L5 is a synthetic peptide composed of 18 amino acids[60] and a molecular weight of 2274 g/mol. L5 carries six positive charges at pH 7.5. The positive charges in all three of these are important for the initial electrostatic attraction of antimicrobial peptides to the negatively charged phospholipid bacterial membranes.

Figure 2 demonstrates the loading capacity of the two different types of hydrogel with lysozyme, peptide L5, and gentamicin. The incorporation of the macromolecules into the film leads to an increase in the dry thickness. The loading ratio

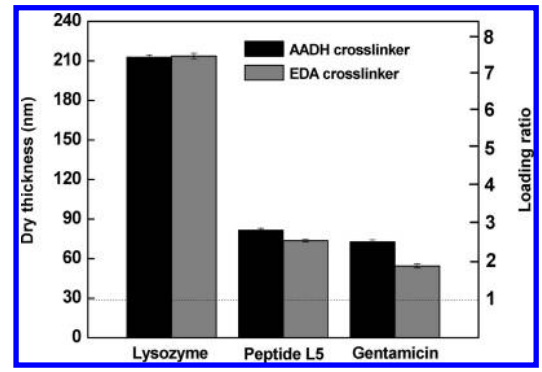

Figure 2. Ellipsometric dry thicknesses of AADH- and EDA-cross-linked $(PMAA)_{10}$ hydrogels after loading lysozyme, L5, and gentamicin in buffer solutions at pH 7.5 (supported by 0.01 M phosphate buffer). The dotted horizontal line indicates the dry thickness of as-synthesized hydrogel. The precursor layer thickness of 9 nm has been subtracted from all data. Dry thickness of 1 nm corresponds to 1 mg/m^2 of organic coating.

is defined as the ratio of dry hydrogel thickness after loading agents to that of the hydrogels prior to loading. The precursor layer thickness of 9 nm has been subtracted from all data. Hydrogels cross-linked with AADH and EDA absorb the same amount of lysozyme, showing a 7.3-fold increase in thickness after lysozyme loading. For gentamicin and L5 loading within EDA-cross-linked hydrogel, the thickness increases were significantly smaller, that is, ~2.1- and ~2-fold. The amount of loaded AmA decreased from lysozyme to L5 and gentamicin, following the charge neutralization rule. The mass per charge within the film was 1825 g/mol-charge for lysozyme, 380 g/mol-charge for peptide L5, and 160 g/mol-charge for gentamicin. Hydrogen bonding between -C(O)-NH- groups and amide groups of L5 or -Ö- or -OH groups of gentamicin is likely to occur. These additional bonds may explain the slightly higher loading of peptide L5 and gentamicin into AADH-cross-linked hydrogels. The antimicrobials were retained in the films after rinsing with 0.01 M phosphate buffer in the absence of extra salt with the same pH as that used for loading.

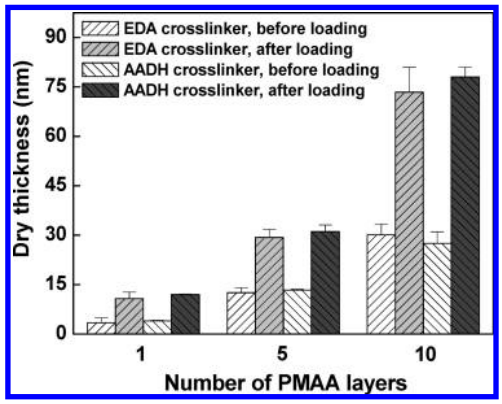

Figure 3. Loading of L5 with PMAA hydrogels, shown as an increase in ellipsometric dry thickness of the PMAA hydrogels cross-linked with EDA and AADH cross-linkers as a function of hydrogel thickness. The precursor layer thickness of 9 nm has been subtracted from all data. Dry thickness of 1 nm corresponds to 1 mg/m^2 of organic coating.

The loading capacity of L5 in each of the two types of hydrogels was also studied using ellipsometry as a function of the hydrogel thickness (Figure 3). The amount loaded was calculated from the difference of the hydrogel thickness before and after loading. Importantly, twice the amount of L5 was loaded within 10-layer PMAA hydrogel films as compared to 5-layer PMAA hydrogel films (4 and 2 μg/cm^2, respectively), suggesting that incorporation of L5 occurs across the entire film thickness. Assuming the persistent length of 5 Å and Gaussian statistics of the random coil, the size of peptide L5 is calculated to be ~1.5 nm. The fact that the L5 size is significantly smaller than an estimated value of the hydrogel mesh size of ~3.4 nm (see above) enables penetration and homogeneous loading of L5 within the hydrogel. A similar linear increase in the loaded amount with the film thickness was also observed for a much smaller molecule of gentamicin (data not shown).

AmA Release as a Function of Ionic Strength and pH. After incorporation of the guest molecules within the hydrogel, the effect of the hydrogel composition on the retention of AmAs within hydrogels in salt solutions and various pH values was investigated.

Ionic Strength Triggered Release. Figure 4 compares the retention of lysozyme, gentamicin, and L5 within the hydrogels as a function of salt concentration at the constant pH value of 7.5. The fraction of AmA released in solution (obtained from ellipsometric measurements of dry AmA-loaded PMAA hydrogels) is plotted as a function of the sodium chloride concentration. The film thickness decreased in salt solutions due to the dissociation of ionic pairs between the -COO^- groups of PMAA and the -NH_3^+ groups of the AmAs. Of specific interest are the physiologically relevant ionic strengths from 0.15 to 0.2 M NaCl. While lysozyme/hydrogel ionic contacts completely dissociated in 0.2 M NaCl solutions at pH 7.5, ~70% and more than 70% of gentamicin and L5, respectively, were retained within the hydrogels. Moreover, L5 showed different retention within EDA-cross-linked and AADH-cross-linked matrices. In 0.2 M NaCl, EDA-cross-linked hydrogel released ~15% of its L5, while AADH-cross-linked hydrogel released none. Such a difference is due to the additional hydrogen bonding between L5 and AADH. Furthermore, the retention was long-term, that is, the amount released reached a limit after 2 h and did not increase beyond that during the following 6 days.

pH-Triggered Release. We then explored the effect of pH on the retention of AmAs within PMAA hydrogels. During these experiments, the ionic strength was kept at 0.2 M NaCl. Because

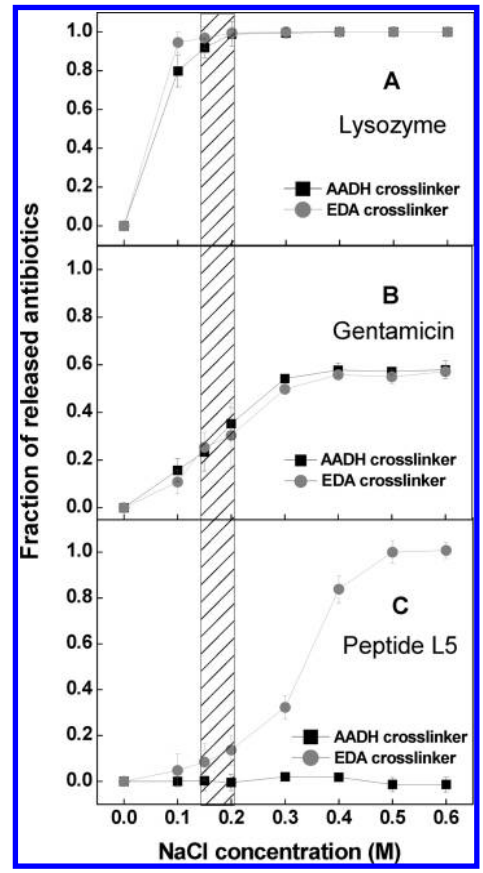

Figure 4. Effect of ionic strength on the release of lysozyme (A), gentamicin (B), and peptide L5 (C) from $(PMAA)_{10}$ hydrogels at pH 7.5. Ellipsometric thicknesses of dry AmA-loaded PMAA hydrogels after a 20 min exposure to salt solutions, required for completion of AmA release, were used in the calculation of fraction released. All error bars represent the standard deviation obtained from three separate experiments.

the lysozyme was not retained within the hydrogel matrix at this salt concentration (Figure 4), further experiments were performed only with gentamicin and peptide L5. Figure 5 shows the retained amount of gentamicin and peptide L5 with decreasing pH supported by 0.01 M phosphate buffer with 0.2 M NaCl. The hydrogels were loaded with AmAs in 0.01 M phosphate buffer at pH 7.5 in the absence of additional NaCl. Each measurement of release was done after soaking the samples in 0.2 M NaCl solution at a specific pH for 20 min, rinsing carefully with buffer of the same pH without NaCl, and then drying with nitrogen. Figure 4 shows that a fraction of gentamicin (~0.2−0.4) released at pH 7.5 is due to the increased ionic strength. Further lowering pH to 5 resulted in the complete release of gentamicin from the EDA-cross-linked $(PMAA)_{10}$ hydrogel, and ~80% release from the AADH-cross-linked PMAA hydrogel. Retention of L5 within both types of hydrogels was much stronger, and drastic differences between the two matrixes were evident. For example, the percentage of peptide released at pH 5 was ~90 and 15% for the EDA- and AADH-cross-linked hydrogels, respectively. The different retentions can be attributed to the formation of >C═O···H−N< hydrogen bonds between the amide motifs of L5 and those of AADH.[67,68] The kinetics of L5 release from EDA- and AADH-cross-linked $(PMAA)_{10}$ hydrogels is shown in Figure S3 in the Supporting Information. Because the L5 demonstrated higher retention within the hydrogels at pH 7.5, our further work was exclusively focused on the peptide-loaded hydrogels. The two types of L5-

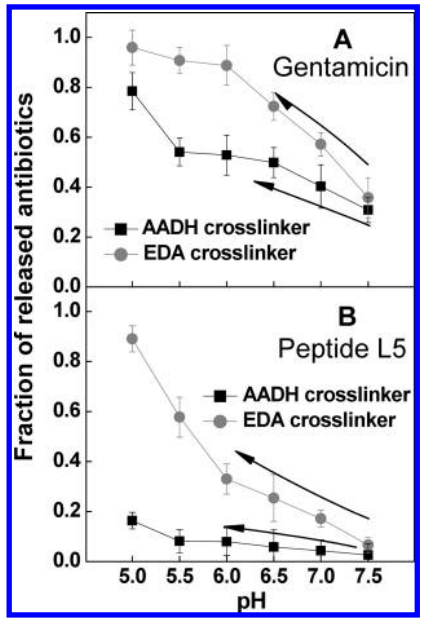

Figure 5. Effect of pH on retention of peptide L5 from EDA- and AADH-stabilized $(PMAA)_{10}$ hydrogels. The fraction released was determined as the ratio of ellipsometric thickness of peptide-loading after pH-triggered release into 0.01 M phosphate buffer containing 0.2 M NaCl thickness to the thickness of antibiotics loaded into $(PMAA)_{10}$ films at pH 7.5. All error bars represent the average standard deviation obtained from three separate experiments.

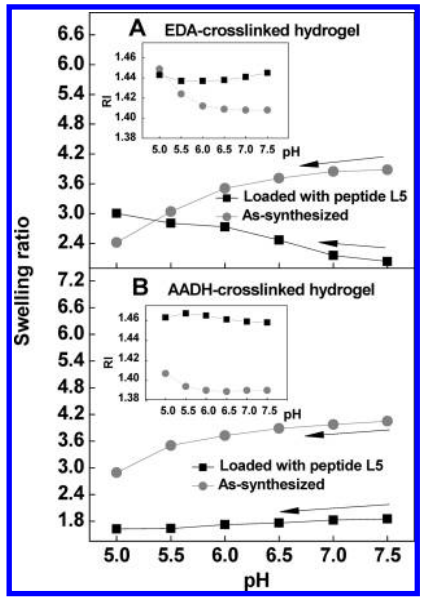

Figure 6. In situ ellipsometry study of the pH effect on swelling of as-synthesized and L5-loaded hydrogels containing EDA (A) or AADH (B) cross-linkers. Insets show the refractive indices (RI) of as-synthesized and peptide-loaded hydrogels. The initial dry thickness of EDA- and AADH-cross-linked $(PMAA)_{10}$ hydrogels after subtraction of the precursor layer contribution was 32 nm. The concentration of NaCl was 0.2 M.

absorbing hydrogels present two extreme cases of pH-responsive and pH-insensitive matrices.

To understand the effect of L5 loading and release on the swelling of PMAA hydrogels, in situ ellipsometry measurements were performed. The results are shown in Figure 6. As-synthesized EDA- or AADH-cross-linked hydrogels were highly swollen at pH 7.5, and their swelling ratio decreased as the pH was decreased from 7.5 to 5. In contrast, L5-loaded hydrogels were much less swollen (and had a high refractive index)

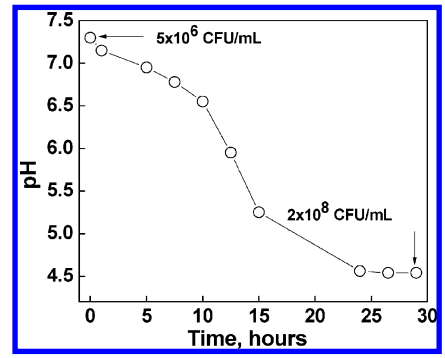

Figure 7. pH variation during growth of *S. epidermidis* in TSB.

because of the neutralization of PMAA charge by the absorbed peptide. EDA-cross-linked hydrogel swelled, however, while releasing its load. AADH-cross-linked hydrogels did not show any changes in swelling upon lowering the pH, as it strongly retained its loaded L5. Therefore, we have obtained two types of peptide-loaded PMAA hydrogels, which show drastically different capabilities to retain/release antibacterial peptide in response to pH variation.

pH Evolution during Growth of *S. epidermidis* in Solution. To study the growth of bacteria over time and to monitor the corresponding changes in solution pH, 50 μL of bacterial inoculum (10^8 CFU/mL) were incubated in 2 mL of TSB for various periods of time. After 24 h, the bacterial concentration increased 24-fold, reaching 2×10^8 CFU/mL. Figure 7 shows that during proliferation under static culture conditions, *S. epidermidis* creates an acidic environment, which can be attributed to the metabolic production of lactic acid.[69]

***S. epidermidis* in Contact with Peptide-Loaded Hydrogels.** We then studied the growth of planktonic *S. epidermidis* in the presence of both as-synthesized and L5-loaded hydrogels. After 4 h of incubation at 37 °C, the pH of the nutrient-rich medium containing *S. epidermidis* decreased to 7. As shown in Figure 5, ~20% of the peptide L5 loaded in EDA-cross-linked hydrogel should be released in the surrounding solution under such conditions, while no L5 was released from AADH-cross-linked hydrogel.

Figure 8 compares the effect of as-synthesized and L5-loaded hydrogels on the growth of *S. epidermidis* in solution (panel A) with bacterial attachment at the hydrogel surface (panel B). In panel A, antibacterial activity of the L5 released from EDA-cross-linked hydrogel was quantified by measuring the optical density at 600 nm of the culture medium in contact with hydrogel-coated silicon and normalizing these values to the optical density measured from medium where *S. epidermidis* was cultured in the absence of hydrogel-coated wafers. A ~40% inhibition of bacterial growth occurred exclusively in the case when bacterial solution was in contact with L5-loaded EDA-cross-linked hydrogel. Importantly, the antimicrobial efficacy of L5 was retained after its release from the EDA-cross-linked hydrogels (Figure 8, panel A). An incomplete inhibition of bacterial growth in solution occurred since the total amount of loaded L5 in the experiment was only ~10% the L5's MIC toward *S. epidermidis* of 20 μM (45 μg/mL). However, the amount of loaded antibacterial agent can be increased by simply increasing the hydrogel thickness. Consistent with Figure 5, AADH-cross-linked hydrogels did not release L5 into solution (Figure 8, panel A).

Panel B in Figure 8 shows the surface coverage of as-synthesized and L5-loaded hydrogels by *S. epidermidis* after 4 h of incubation. The data in Figure 8 are calculated from the

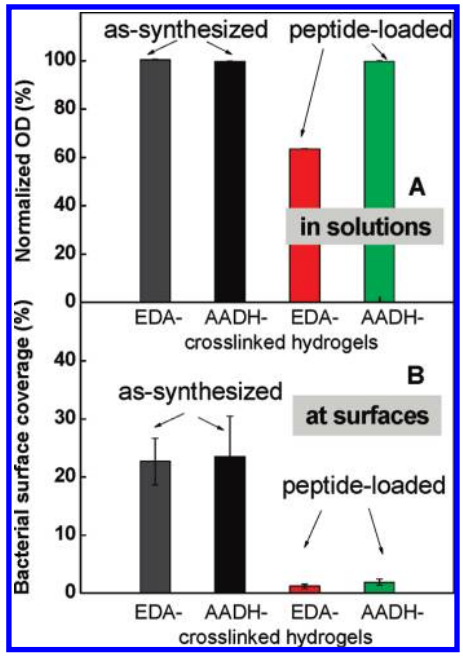

Figure 8. Growth of *S. epidermidis* in the presence of the as-synthesized and L5-loaded $(PMAA)_{10}$ hydrogels. Panel A: Normalized OD_{600} of *S. epidermidis* in TSB after incubation for 4 h in the presence of the as-synthesized or peptide-loaded hydrogels. The normalization was done relative to the absorbance of the hydrogel-free bacterial growth in TSB. Panel B: Surface coverage of *S. epidermidis* after incubation for 4 h in the TSB medium. All error bars represent the average standard deviation obtained from three separate experiments.

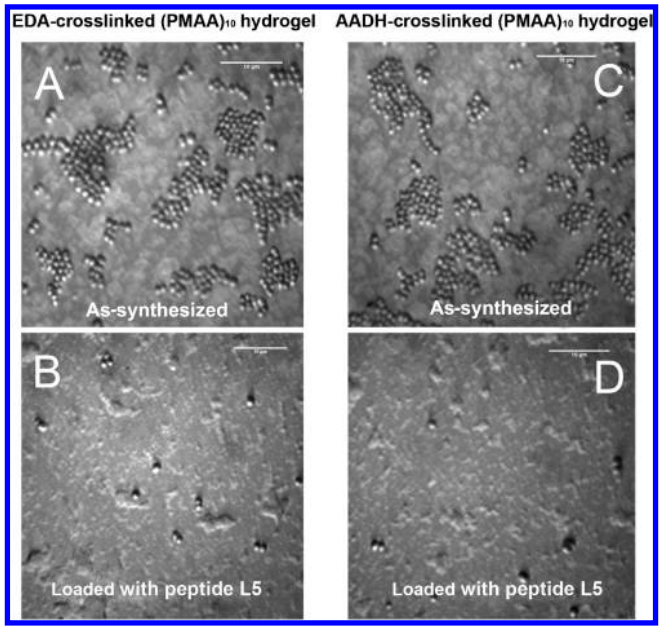

Figure 9. Representative optical images of $(PMAA)_{10}$ films exposed to 10^7 CFU/mL *S. epidermidis* in TSB for 4 h: Panel A, EDA-cross-linked hydrogel; Panel B, EDA-cross-linked hydrogel loaded with peptide L5; Panel C, AADH-cross-linked hydrogel; and Panel D, AADH-cross-linked hydrogel loaded with peptide L5. Scale bar is 10 μm.

optical images (representative images are shown in Figure 9) using Adobe Photoshop. A significant amount of bacteria was observed after 4 h of *S. epidermidis* culture on as-synthesized EDA- and AADH-cross-linked hydrogels. This result is somewhat surprising, considering the high swelling ratio of such hydrogels (Figure 1) and the capacity of many hydrogels to resist cellular and bacteria adhesion.[70] In contrast, L5-loaded $(PMAA)_{10}$ films showed almost complete inhibition of bacterial colonization (Figure 9B,D). These experiments demonstrate that L5 included within the hydrogel preserved its antibacterial activity, acting against *S. epidermidis* bacteria upon their contact with the surface.

Conclusions and Outlook

We have shown that functionalizing surfaces with antimicrobial-absorbing hydrogel thin films presents an effective way to produce a new family of antibacterial coatings. The PMAA-based hydrogel films we studied offer an electrostatic mechanism with which to absorb and retain polycationic antimicrobial substances. Using gentamicin and an antimicrobial peptide derived from lactoferrin, we demonstrated that these antimicrobial substances can be released from the PMAA hydrogel thin films in response to changes of pH and salt concentration in the surrounding medium. Importantly, we were able to further tune antimicrobial release by varying the type of cross-linker. Specifically, the use of AADH as a cross-linker supplies centers for hydrogen bonding, and, relative to the films cross-linked by EDA, increases the retention of loaded antibacterial peptides at high concentrations of salts and at low pH values. Peptide-loaded EDA- and AADH-cross-linked hydrogels represent two extreme cases of pH-responsive and pH-insensitive matrices. Antibacterial activity of these two types of peptide-loaded hydrogels was demonstrated using experiments with the gram-positive bacterium *S. epidermidis*. While both types of peptide-loaded hydrogels strongly inhibit bacterial colonization at surfaces, EDA-cross-linked matrices provide the additional benefit of killing bacteria in solution in response to bacterial growth in the medium surrounding the synthetic surface. The possibility of tuning the loading capacity, drug retention, and pH-dependent release profiles of therapeutic agents from surface-bound hydrogel matrices has important implications for the development of advanced antibacterial coatings with tailored loading capacity and release characteristics.

Acknowledgment. This research project has been supported by the National Science Foundation through Grant No. CBET-0708379. The authors are grateful to Prof. James Liang at Stevens for his helpful discussions and help with our preliminary peptide L5 experiments.

Supporting Information Available. Ellipsometric thicknesses and ATR-FTIR data on PVPON/PMAA films before and after PVPON release, and kinetics of L5 release from EDA- and AADH-cross-linked $(PMAA)_{10}$ hydrogels determined by ellisopmetry. This material is available free of charge via the Internet at http://pubs.acs.org.

References and Notes

(1) Parvizi, J.; Azzam, K.; Ghanem, E.; Austin, M. S.; Rothman, R. H. *Clin. Orthop. Relat. Res.* **2009**, *467*, 1732.
(2) Campoccia, D.; Montanaro, L.; Arciola, C. R. *Biomaterials* **2006**, *27*, 2331.
(3) Costerton, J. W.; Stewart, P. S.; Greeenberg, E. P. *Science* **1999**, *284*, 1318.
(4) Watnick, P.; Kolter, R. *J. Bacteriol.* **2000**, *182*, 2675.
(5) Costerton, J. W. In *Microbial Biofilm*; Ghannoum, M., O'Toole, G. A., Eds.; ASM Press: Washington, D.C., 2004.
(6) Costerton, J. W. *Clin. Orthop. Relat. Res.* **2005**, *437*, 7.
(7) Jenkinsn, H. F.; Lappin-Scott, H. M. *Trends Microbiol.* **2001**, *9*, 9.
(8) Gristina, A. G.; Hobgood, C. D.; Webb, L. X.; Myrvik, Q. N. *Biomaterials* **1987**, *8*, 423.
(9) Rodriguez-Martinez, J. M.; Pascual, A. *Rev. Med. Microbiol.* **2006**, *17*, 65.
(10) Klibanov, A. M. *J. Mater. Chem.* **2007**, *17*, 2479.

(11) Mukherjee, K.; Rivera, J. J.; Klibanov, A. M. *Appl. Biochem. Biotechnol.* **2008**, *151*, 61.
(12) Tang, H.; Wang, A.; Liang, X.; Cao, T.; Salley, S. O.; McAllister, J. P., III; Ng, K. Y. S. *Colloids Surf., B* **2006**, *51*, 16.
(13) Cao, Z.; Sun, Y. *Appl. Mater. Interfaces* **2009**, *1*, 494.
(14) Kenawy, E.-R.; Worley, S. D.; Broughton, R. *Biomacromolecules* **2007**, *8*, 1359.
(15) Yu, D. G.; Lin, W. C.; Yang, M. C. *Bioconjugate Chem.* **2007**, *18*, 1521.
(16) Cunliffe, D.; de las Heras Alarsón, C.; Peters, V.; Smith, J. R.; Alexander, C. *Langmuir* **2003**, *19*, 2888.
(17) Bridges, A. W.; Garcia, A. J.; Lyon, L. A. *Biomacromolecules* **2007**, *8*, 3271.
(18) Richert, L.; Lavalle, P.; Payan, E.; Shu, X. Z.; Prestwich, G. D.; Stoltz, J.-F.; Schaaf, P.; Voegel, J.-C.; Picart, C. *Langmuir* **2004**, *20*, 448.
(19) Fu, J.; Ji, J.; Yuan, W.; Shen, J. *Biomaterials* **2005**, *26*, 6684.
(20) Ji, J. F. A.; Fan, D.; Shen, J. *J. Biomed. Mater. Res. A* **2006**, *79*, 665.
(21) Mao, Z.; Ma, L.; Gao, C.; Shen, J. *J. Controlled Release* **2005**, *104*, 193.
(22) Madkour, A. E.; Dabkowsli, J. M.; Nüsslein, K.; Tew, G. N. *Langmuir* **2009**, *25*, 1060.
(23) Nguyen, P. M.; Zacharia, N. S.; Verploegen, E.; Hammond, P. T. *Chem. Mater.* **2007**, *19*, 5524.
(24) Boddohi, S.; Killingsworth, C. E.; Kipper, M. J. *Biomacromolecules* **2008**, *9*, 2021.
(25) Elzbieciak, M.; Zapotoczny, S.; Nowak, P.; Krastev, R.; Nowakowska, M.; Warszyñski, P. *Langmuir* **2009**, *25*, 3255.
(26) Guyomard, A.; Deì, E.; Jouenne, T.; Malandain, J. J.; Muller, G.; Glinel, K. *Adv. Funct. Mater.* **2008**, *18*, 758.
(27) Litcher, J. A.; Thompson, M. T.; Delgadillo, M.; Nishikawa, T.; Rubner, M. F.; Van Viet, K. J. *Biomacromolecules* **2008**, *9*, 1571.
(28) Thompson, M. T.; Berg, M. C.; Tobias, I. S.; Lichter, J. A.; Rubner, M. F.; Van Vliet, K. J. *Biomacromolecules* **2006**, *7*, 1990.
(29) Grunland, J. C.; Choi, J. K.; Lin, A. *Biomacromolecules* **2005**, *6*, 1149.
(30) Kim, B. S.; Park, S. W.; Hammond, P. T. *ACS Nano* **2008**, *2*, 386.
(31) Nguyen, P. M.; Hammond, P. T. *Langmuir* **2006**, *22*, 7825.
(32) Laugel, N.; Hemmerlé, J.; Ladhari., N.; Arntz, Y.; Gonthier, E.; Haikel, Y.; Voegel, J. C.; Ball, V. *J. Colloid Interface Sci.* **2008**, *324*, 127.
(33) Chuang, H. F.; Smith, R. C.; Hammond, P. T. *Biomacromolecules* **2008**, *9*, 1660.
(34) Moskowitz, J. S.; Blaisse, M. R.; Samuel, R. E.; Hsu, H.-P.; Harris, M. B.; Martin, S. D.; Lee, J. C.; Spector, M.; Hammond, P. T. *Biomaterials* **2010**, *31*, 6019.
(35) Nepal, D.; Balasubramanian, S.; Simonian, A. L.; Davis, V. A. *Nano Lett.* **2008**, *8*, 1896.
(36) Chua, P.-H.; Neoh, K.-G.; Kang, E.-T.; Wang, W. *Biomaterials* **2008**, *29*, 1412.
(37) Li, Z.; Lee, D.; Sheng, X.; Cohen, R. E.; Rubner, M. F. *Langmuir* **2006**, *22*, 9820.
(38) Fu, J.; Ji, J.; Fan, D.; Shen, J. *J. Biomed. Mater. Res.* **2006**, *79*, 665.
(39) Ji, J.; Fu, J.; Shen, J. *J. Biomed. Mater. Res. B* **2008**, *85*, 556.
(40) Shai, Y. *Biopolymer* **2002**, *66*, 236.
(41) Brogden, K. A. *Nat. Rev. Microbiol.* **2005**, *3*, 238.
(42) Singh, P. K.; Parsek, M. R.; Greenberg, E. P.; Welsh, M. J. *Nature* **2002**, *417*, 552.
(43) Hancock, R. E. W.; Diamond, G. *Trends Microbiol.* **2000**, *8*, 402.
(44) Etienne, O.; Picart, C.; Taddei, C.; Haikel, Y.; Dimarcq, J. L.; Schaaf, P.; et al. *Antimicrob. Agents Chemother.* **2004**, *48*, 3662.
(45) Etienne, O.; Gasnier, C.; Taddei, C.; Voegel, J.-C.; Aunis, D.; Schaaf, P.; et al. *Biomaterials* **2005**, *26*, 6704.
(46) Shukla, A.; Fleming, K. E.; Chuang, H. F.; Chau, T. M.; Loose, C. R.; Stephanopoulos, G. N.; Hammond, P. T. *Biomaterials* **2010**, *31*, 2348.
(47) Kozlovskaya, V.; Kharlampieva, E.; Erel, I.; Sukhishvili, S. A. *Soft Matter* **2009**, *5*, 4077.
(48) Stuart, M. A. C.; Huck, W. T. S.; Genzer, J.; Müller, M.; Ober, C.; Stamm, M.; Sukhorukov, G. B.; Minko, S. *Nat. Mater.* **2010**, *9*, 101.
(49) Liu, F.; Urban, M. W. *Prog. Polym. Sci.* **2010**, *35*, 3.
(50) Chung, A. J.; Rubner, M. F. *Langmuir* **2002**, *18*, 1176.
(51) Jiang, B.; Barnett, J. B.; Li, B. *Nanotechnol., Sci. Appl.* **2009**, *2*, 27.
(52) Jiang, B.; Li, B. *Int. J. Nanomed.* **2009**, *4*, 37.
(53) Kharlampieva, E.; Erel-Unal, I.; Sukhishvili, S. A. *Langmuir* **2007**, *23*, 175.
(54) Branda, S. S.; Vik, A.; Friedman, L.; Kolher, R. *Trends Microbiol.* **2005**, *13*, 20.
(55) Sutherland, I. W. *Trends Microbiol.* **2001**, *9*, 222.
(56) Mack, D. *J. Hosp. Infect.* **1999**, *43*, 113.
(57) Kaplan, J. B.; Ragunath, C.; Velliyagounder, K.; Fine, D. H.; Ramasubbu, N. *Antimicrob. Agents Chemother.* **2004**, *48*, 2633.
(58) Pristinski, D.; Kozlovskaya, V.; Sukhishvili, S. *J. Opt. Soc. Am. A* **2006**, *23*, 2639.
(59) Andrews, J. M. *J. Antimicrob. Chemother.* **2001**, *48*, 5.
(60) Yang, N.; Rekdal, Ø.; Stensen, W.; Svendsen, J. S. *J. Pept. Res.* **2002**, *60*, 187.
(61) Shafer, D. E.; Toll, B.; Schuman, R. F.; Nelson, B. L.; Mond, J.; Lees, A. *Vaccine* **2000**, *18*, 1273.
(62) Erel-Unal, I.; Sukhishvili, S. A. *Macromolecules* **2008**, *41*, 3962.
(63) Kozlovskaya, V.; Kharlampieva, E.; Mansfield, M. L.; Sukhishvili, S. A. *Chem. Mater.* **2006**, *18*, 328.
(64) Wang, Z.; Li, D.; Jim, J. *Spectrochim. Acta* **2008**, *70*, 866.
(65) Gao, G.; Yao, P. *J. Polym. Sci., Polym. Chem.* **2008**, *46*, 4681.
(66) Smith, A. L.; Daum, R. S.; Siber, G. R.; Scheifele, D. W.; Syriopoulou, V. P. *Antimicrob. Agents Chemother.* **1988**, *32*, 1034.
(67) Ueyama, N.; Takahashi, K.; Onoda, A.; Okamura, T.; Yamamoto, H. *J. Biotechnol.* **2007**, *127*, 670.
(68) Lynch, I.; Blute, I. A.; Zhmud, B.; MacArtain, P.; Tosetto, M.; Allen, L. T.; Byrne, H. J.; Dawson, K. A. *Chem. Mater.* **2005**, *17*, 3889.
(69) Handke, L. D.; Rogers, K. L.; Olson, M. E.; Somerville, G. A.; Jerrells, T. J.; Rupp, M. E.; Dunman, P. M.; Fey, P. D. *Infect. Immun.* **2008**, *76*, 141.
(70) Krsko, P.; Kaplan, J. B.; Libera, M. *Acta Biomater.* **2009**, *5*, 589.

BM100975W